PHYSICAL REVIEW B **83**, 100408(R) (2011)

Compact merons and skyrmions in thin chiral magnetic films

Motohiko Ezawa
Department of Applied Physics, University of Tokyo, Hongo 7-3-1, 113-8656, Japan
(Received 20 February 2011; published 18 March 2011)

A meron is a controversial topological excitation because it carries just one-half of the skyrmion number. A vortex in thin magnetic films has been argued to be a half-skyrmion, i.e., a meron. We present another type of merons, investigating the two-dimensional nonlinear sigma model together with the Dzyaloshinskii-Moriya interaction. Here, the vortex number of a meron is zero. Basic topological excitations are merons and skyrmions. They behave as if they were free particles. A prominent feature is that the topological charge density is strictly confined within compact domains. We propose an analytic approach for these compact excitations, and construct a phase diagram. It is comprised of the helix, meron, skyrmion-crystal, skyrmion-gas, and ferromagnet phases. It captures the essential nature of the experimental data recently performed in chiral magnets such as MnSi and FeCoSi thin films.

DOI: 10.1103/PhysRevB.83.100408 PACS number(s): 75.70.Tj, 73.43.Lp, 11.10.Lm

Topological excitations are endlessly fascinating. Well-known examples are vortices and skyrmions.[1] A fantastic object is a meron: it can not exist by itself since it carries only one-half of the skyrmion number. A meron was originally invented as a half-instanton in the context of quark confinement in particle physics.[2] Then, it was introduced as a half-skyrmion in order to account for a certain anomalous behavior in bilayer quantum Hall effects.[3] Later, a meron was shown to appear as a vortex in magnetic thin films,[4,5] where an annihilation of a meron pair was analyzed numerically.[6] A meron carries one unit of the vortex number and one-half of the skyrmion number in these systems.[3–6]

Recently, a skyrmion crystal[7] as well as a single skyrmion[8] have been observed experimentally in chiral magnets such as MnSi and FeCoSi thin films. Furthermore, magnetic domains observed in ferromagnets such as a TbFeCo thin film[9] have been argued to be giant skyrmions[10] as large as $\sim 1\,\mu$m. In this paper, we point out that there exist also merons in chiral magnets and that they have already been observed.

The ground state of chiral magnets is a helical state in the absence of external magnetic field. The spin texture of the helical state has a stripe-domain structure, where the width of a stripe has a fixed value determined by sample parameters. A stripe breaks into pieces as the magnetic field increases. By calculating the topological charge density, we show that the endpoint of a broken stripe has the skyrmion number $Q_{\rm sky} = 1/2$. However, the vortex number is zero: $Q_{\rm vortex} = 0$. A finite-length stripe is a bimeron (a pair of merons) (Fig. 1), which has the same topological number as a skyrmion.

When we talk about skyrmions in the two-dimensional space, it is implicit to assume a Belavin-Polyakov skyrmion. Its spin texture approaches the ground-state value only polynomially at large distances. On the contrary, a skyrmion must be strictly compact in the chiral magnet since it is embedded within a stripe-domain structure. We propose an analytic scheme to explore compact merons and skyrmions. They behave as if they were almost free particles. Based on this observation, using a simple combinatorial analysis, we construct a phase diagram of the chiral ferromagnet. It captures the essential nature of the phase diagram obtained experimentally in a FeCoSi thin film.[8] This shows that our treatment of merons as free particles is approximately correct in the chiral magnet.

Our system is the two-dimensional plane described by the nonlinear $O(3)$ sigma model H_J with easy axis anisotropy,

$$H_J = \frac{1}{2}\Gamma \int d^2x\, [(\partial_k \boldsymbol{n})(\partial_k \boldsymbol{n}) - \xi^{-2}(n_z)^2], \tag{1}$$

and the Dzyaloshinskii-Moriya interaction (DMI)

$$H_{\rm DM} = D \int d^2x\, \boldsymbol{n}(\boldsymbol{x}) \cdot [\nabla \times \boldsymbol{n}(\boldsymbol{x})], \tag{2}$$

where Γ is the exchange energy, ξ is the single-ion easy-axis anisotropy constant, and $\boldsymbol{n} = (n_x, n_y, n_z)$ is a classical spin field of unit length. The DMI term breaks the chiral symmetry explicitly. We introduce the magnetic field h perpendicular to the plane with the Zeeman energy $\Delta_Z = Sg\mu_B\mu_0 h$:

$$H_Z = -(\Delta_Z/a^2) \int d^2x\, n_z(\boldsymbol{x}), \tag{3}$$

where a is the lattice constant.

We have emphasized previously[10] the importance of the magnetic dipole-dipole interaction (DDI). However, since the

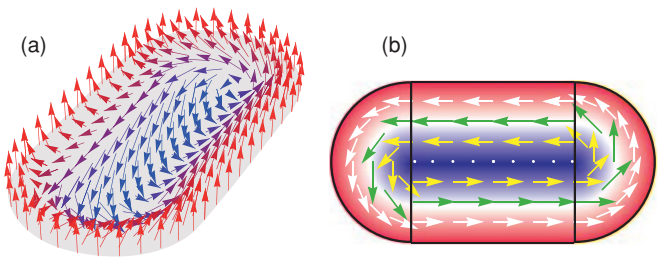

FIG. 1. (Color online) (a) The spin texture of a compact bimeron in a thin chiral magnetic film. (b) A compact bimeron is composed of two half-disk domains and a rectangular stripe domain. Spins are pointed upward on the boundary and downward deep inside of the bimeron. They are pointed forward and backward in the rectangular part, and twisting circularly in the half-disk part. The topological charge density is nonvanishing only in the half-disk parts, each of which has $Q_{\rm sky} = 1/2$. The half-disk part is identified as a meron. The spin texture of a compact skyrmion is obtained simply by removing the rectangular part and by patching the two half-disk domains.

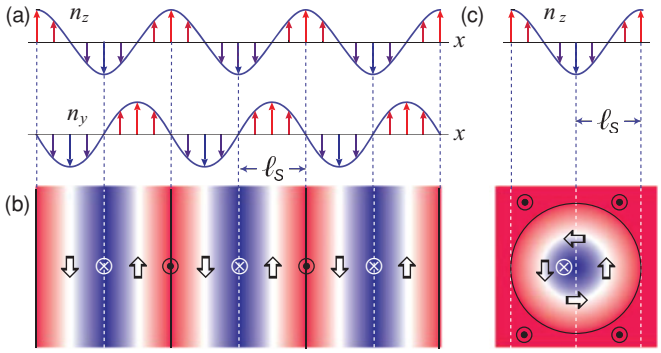

FIG. 2. (Color online) (a) Illustration of the helical state solution $n_i(x)$ described by the Jacobian elliptic function (5). Here we have taken $\kappa = 0.3$. (b) Illustration of the spin structure with an alternating up-down and forward-backward stripe domain. Spins are strictly pointed up or down on the vertical solid or dotted lines. As one stripe, we consider the region sandwiched by two solid lines. (c) Illustration of a compact skyrmion described by the Jacobian elliptic function (8). It is constructed in such a way that any cross section passing through the center agrees with the cross section of the stripe. The topological charge is strictly confined within the solid circle.

DDI constant is very small compared to the DMI constant, we may ignore it in determining the magnetic structure of a chiral magnet. Indeed, the typical size determined by the DMI is of the order of 40 nm, where the DDI is negligible.

We start with a study of the system in the absence of external magnetic field. The ferromagnetic spin state $\boldsymbol{n} = (0,0,\pm 1)$ is a solution of the Hamiltonian $H_{J\text{-DM}} = H_J + H_{\text{DM}}$ with the energy density

$$E_{\text{homo}} = -\Gamma/2\xi^2. \tag{4}$$

However, in general, this is not the ground state. It is easy to prove that the Hamiltonian $H_{J\text{-DM}}$ allows one-dimensional periodic solutions, among which is the one that minimizes the DMI term (2) given by

$$\begin{aligned} n_x(x) = 0, \quad n_y(x) = \text{cn}\left(\frac{x-\ell_S/2}{\kappa\xi},\kappa^2\right), \\ n_z(x) = \text{sn}\left(\frac{x-\ell_S/2}{\kappa\xi},\kappa^2\right) \end{aligned} \tag{5}$$

in terms of the Jacobian elliptic functions [Fig. 2(a)], where κ is an integration constant with $0 \leqslant \kappa^2 \leqslant 1$. The periodicity of $\sigma(x)$ is $2\ell_S \equiv 4\kappa\xi K(\kappa^2)$, where $K(\kappa^2)$ is the complete elliptic integral of the first kind. The periodic state (5) has an alternating up-down and forward-backward spin-stripe structure, as illustrated in Fig. 2(b). It may be called the anisotropic helical state. Note that $n_z(-\ell_S) = 1$, $n_z(0) = -1$, and $n_z(\ell_S) = 1$. As one stripe, we consider the region, the width of which is $2\ell_S$ with the center line being given by $n_z(x) = -1$.

By substituting (5) into the Hamiltonian $H_{J\text{-DM}}$, the energy density of the helical state is analytically calculable:

$$E_{\text{helix}} = \frac{\Gamma}{2\xi^2}\left(\frac{2}{\kappa^2}\frac{E(\kappa^2)}{K(\kappa^2)} - \frac{1}{\kappa^2} + 1\right) - \frac{\pi D}{2\kappa\xi K(\kappa^2)}. \tag{6}$$

We determine the parameter κ by minimizing E_{helix} with respect to κ. It is given by solving $2E_{\text{helix}}(\kappa^2) = \kappa\pi D\xi/\Gamma$. Provided $D\xi \gg \Gamma$, it is solved as $\kappa = \lambda - \lambda^3/4 + \ldots$, with $\lambda = \Gamma/D\xi$, and the energy density of the helical state is

$$E_{\text{helix}} = -\frac{D^2}{2\Gamma} + \frac{\Gamma}{4\xi^2} + \ldots. \tag{7}$$

We compare this with that of the homogeneous state (4). We find that the helical state has a lower energy than that of the homogeneous state if $D\xi > \sqrt{3/2}\Gamma$. It is interesting that the helical state is not realized in the sample when the anisotropy is too large.

We switch on the external magnetic field. The Zeeman effect enforces the increase of the up-spin region. However, it is impossible to increase only the width of the up-spin part of the stripe, which is fixed to be ℓ_S. The simple way is to split a stripe into two stripes, since it increases up-spin region [Fig. 3(a)]. Let us cut one stripe at $y = 0$ and then put a cap so that the spin field on the cross section smoothly approaches the up-spin value at the boundary in order to optimize the energy [Fig. 1(b)]. The spin texture of the cap must be given by

$$\begin{aligned} n_x(r,\theta) &= -\text{cn}\left(\frac{r-\ell_S/2}{\kappa\xi},\kappa^2\right)\sin\theta, \\ n_y(r,\theta) &= \text{cn}\left(\frac{r-\ell_S/2}{\kappa\xi},\kappa^2\right)\cos\theta, \\ n_z(r,\theta) &= \text{sn}\left(\frac{r-\ell_S/2}{\kappa\xi},\kappa^2\right) \end{aligned} \tag{8}$$

for the half-disk region $(r \leqslant \ell_S, 0 \leqslant \theta \leqslant \pi)$ in the cylindrical coordinate, since it agrees with (5) at $y = 0$, where $\cos\theta = 1$.

A stripe may be broken into three stripes with one finite-length stripe [Fig. 3(a)]. The spin structure of a finite-length stripe is illustrated in Fig. 1. The shortest stripe is a cylindrical symmetric domain [Figs. 3(a) and 2(c)], the spin texture of

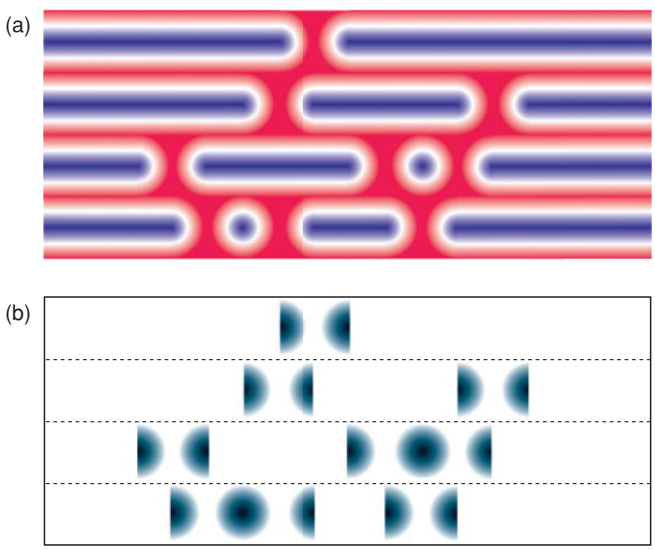

FIG. 3. (Color online) (a) Illustration of compact skyrmions, merons, and bimerons embedded in the stripe-domain structure. (b) Illustration of the topological charge density confined within compact domains. Dotted lines show the boundaries of stripes.

which is described by (8) for the disk region ($r \leqslant \ell_S, 0 \leqslant \theta \leqslant 2\pi$).

The use of a continuum approximation and of classical fields to represent the spins is justified as far as we analyze phenomena with a characteristic wavelength that is much larger than the lattice constant. In this regime, there exists the topologically conserved charge, that is, the Pontryagin number or the skyrmion number $Q_{\rm sky} = \int d^2x\, \rho_{\rm sky}(\boldsymbol{x})$, with

$$\rho_{\rm sky}(\boldsymbol{x}) = -\frac{1}{8\pi}\sum_{ij}\varepsilon_{ij}\boldsymbol{n}(\boldsymbol{x})\cdot[\partial_i\boldsymbol{n}(\boldsymbol{x})\times\partial_j\boldsymbol{n}(\boldsymbol{x})], \tag{9}$$

where i,j run over x,y with ε_{ij} being the completely antisymmetric tensor. We are able to determine the topological charge density $\rho_{\rm sky}(\boldsymbol{x})$ for various spin textures.

First, it is trivial to see that the stripe configuration (5) has no topological density. Then, calculating it for the half-disk configuration (8) with $0 \leqslant \theta \leqslant \pi$, we find that $Q_{\rm sky} = 1/2$. Similarly, we find $Q_{\rm sky} = 1$ for the cylindrical symmetric configuration (8) with $0 \leqslant \theta \leqslant 2\pi$. Clearly, we can identify them as a meron and a skyrmion, respectively. A prominent feature is that the topological charge is strictly confined within a compact domain. Hence, we may call them a compact skyrmion and so on. In general, there appear a variety of topological excitations [Fig. 3(a)]. We have illustrated the corresponding topological charge density in Fig. 3(b). Let us refer to this regime of topological excitations as the meron phase, since the basic excitation is a meron that appears at the endpoint of a stripe. Note that merons are half-vortices.

A comment is in order with respect to the vortex number for the nonlinear sigma field. We can define it by

$$Q_{\rm vortex} = \frac{1}{2\pi}\sum_{ijk}\varepsilon_{ij}\oint dx_k\, n_i(\boldsymbol{x})\partial_k n_j(\boldsymbol{x}), \tag{10}$$

where i,j,k run over x,y. It is given by value of n_i along the boundary of the compact domain, where it follows from (8) that $n_x = 0$. Hence, $Q_{\rm vortex} = 0$ for a meron and a skyrmion in chiral magnet. On the contrary, we find that $Q_{\rm vortex} = \pm 1$ for a vortex-meron[3,5,6] in the easy-plane ferromagnet.

We now estimate the energy of a topological configuration. The Jacobian elliptic functions are well approximated by the sinusoidal functions when κ is not close to 1, say, $\kappa \lesssim 0.5$. Namely, we may approximate (5) by $n_x(x) = 0$, $n_y(x) = \sin(kx)$, and $n_z(x) = -\cos(kx)$, where $k = 1/\kappa\xi$. This is the well-known expression for the helical ground state in the isotropic system, which is the limit $\xi \to \infty$ with k being fixed. The spin texture of the cap (8) is approximated by

$$n_x(r,\theta) = -\sin(kr)\sin\theta, \quad n_y(r,\theta) = \sin(kr)\cos\theta, \quad n_z(r,\theta) = -\cos(kr) \tag{11}$$

for $r \leqslant \pi/k$. We consider the isotropic system for simplicity.

With the use of the meron configuration (11), by integrating the total Hamiltonian $H = H_J + H_{\rm DM} + H_Z$, it is straightforward to calculate the energy gain when a stripe is broken into two stripes:

$$\Delta E_{\rm merons} = \ell_S^2\left[\left(\frac{4}{\sqrt{3}} - \frac{\pi}{2}\right)\frac{D^2}{\Gamma} - \left(\frac{4}{\pi} + \frac{8}{\sqrt{3}} - \pi\right)\Delta_Z\right]. \tag{12}$$

This is the creation energy of a meron pair. The energy gain when a skyrmion emerges in a stripe is just twice of $\Delta E_{\rm merons}$. It follows that $\Delta E_{\rm merons} < 0$ if $\Delta_Z > \Delta_Z^{\text{helix-SkX}}$ with

$$\Delta_Z^{\text{helix-SkX}} = 0.27D^2/\Gamma. \tag{13}$$

Since the energy gain is negative, all stripes are spontaneously broken into a maximum number of skyrmions for $\Delta_Z > \Delta_Z^{\text{helix-SkX}}$, which would lead to the formation of a skyrmion crystal (SkX). Namely, $\Delta_Z^{\text{helix-SkX}}$ is the phase-transition point between the helix and SkX phases. It is concluded that there exists no meron phase at zero temperature.

The SkX has been discussed in literature,[11,12] although Belavin-Polyakov skyrmions are assumed on all lattice points with a certain cutoff.

On the other hand, the ferromagnet (FM) phase appears in sufficiently strong external magnetic field, which has only the Zeeman energy $E_{\rm FM} = -\Delta_Z/a^2$. By comparing this with (12), it follows that the critical Zeeman energy is

$$\Delta_Z^{\text{SkX-FM}} = 0.84D^2/\Gamma, \tag{14}$$

so that the FM phase appears for $\Delta_Z > \Delta_Z^{\text{SkX-FM}}$.

We proceed to construct the phase diagram in the plane of temperature and magnetic field. We have it already at zero temperature, where there exists only the helix, SkX, and FM phases. The meron phase appears at finite temperature, since its entropy is much larger than that of the helix or SkX phase.

At finite temperature, in general, the fluctuation of stripes is important. Indeed, this leads to a labyrinth state of stripes in ordinary ferromagnetic films. However, the real-space imaging experiment and the numerical simulation in Ref. 8 demonstrate clearly that the fluctuation of stripes is small in chiral magnetic films. Instead of fluctuating, a stripe breaks into pieces because there exists an energy gain of the DMI energy. Hence, we neglect it and only take into account the breaking degree of freedom in the first-order approximation.

In determining the boundary between the helix and meron phases, the basic excitation is a pair of merons in the helix phase [Fig. 3(b)]. It appears when a stripe is broken into two pieces with the excitation energy $\Delta E_{\rm merons}$ being given by (12). Let N be the maximum number of the topological charges (the maximum number of compact skyrmions) that the system can accommodate. When the topological charge of the system is n, the entropy is given by $S = \ln N!/n!(N-n)!$. Then, the free energy at temperature T is given by $F = E_{\rm helix} + n\Delta E_{\rm merons} - TS$. Letting $N \to \infty$, we obtain the formula for the free energy density

$$f = \varepsilon_{\rm helix} + q\Delta E_{\rm merons} + \frac{k_{\rm B}T}{2}\left(q - \frac{1}{2}\right)^2, \tag{15}$$

where $f = F/N$, $\varepsilon_{\rm helix} = E_{\rm helix}/N$, and $q = n/N$ is the average topological charge density ($0 \leqslant q \leqslant 1$). It is easy to minimize the free energy density f with respect to q. Since f is quadratic in q, it yields two lines starting from the helix-SkX phase-transition point at $T = 0$. They determine the boundary between the helix-meron phases and the boundary between the meron-SkX phases, as illustrated in Fig. 4. The SkX melts into

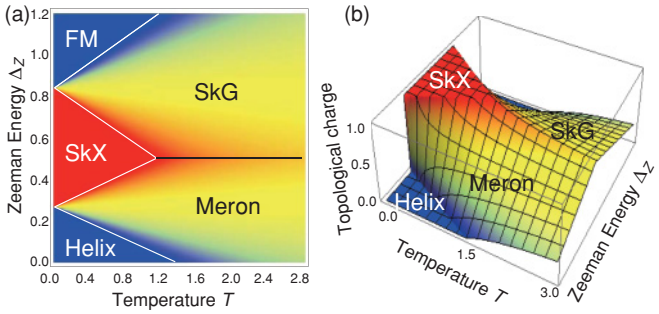

FIG. 4. (Color online) (a) Phase diagram. The horizontal axis is the temperature T in units of $D^2/k_B\Gamma$, while the vertical axis is the Zeeman energy Δ_Z in units of D^2/Γ. (b) Average topological charge density in various phases.

a skyrmion gas (SkG) at higher temperature. We can make a similar argument to derive the boundary between the SkX and SkG phases, where the basic object is a skyrmion in the SkX phase with the excitation energy being

$$\Delta E_{\rm sky} = -\ell_S \left[\frac{\pi D^2}{2\Gamma} + \left(\frac{4}{\pi} - \pi \right) \Delta_Z \right]. \qquad (16)$$

We arrive at the same formula as (15) by replacing $\varepsilon_{\rm helix}$ with $\varepsilon_{\rm SkX}$, and $\Delta E_{\rm merons}$ with $\Delta E_{\rm sky}$. In this way, we obtain the boundary between the SkX-SkG phases and the boundary between the SkG-FM phases [Fig. 4]. Finally, the boundary between the meron and SkG phases is given by $\Delta_Z^{\text{meron-SkG}} = D^2/2\Gamma$ for $T > 4D^2/\pi k_B\Gamma$ by comparing their free energies.

The phase diagram thus constructed is characterized by the topological charge density q as follows:

$$q = \begin{cases} 0 & \text{for} \Delta E_i > \frac{1}{2}k_BT \quad \text{(helix, FM)}, \\ \frac{1}{2} - \frac{\Delta E_i}{T} & \text{for} |\Delta E_i| < \frac{1}{2}k_BT \quad \text{(meron, SkG)}, \\ 1 & \text{for} -\Delta E_i > \frac{1}{2}k_BT \quad \text{SkX}, \end{cases} \qquad (17)$$

where ΔE_i stands for $\Delta E_{\rm merons}$ or $\Delta E_{\rm sky}$. Note that the topological charge density q is observable by measuring the Hall conductance σ_{xy} of the topological current[13–15] $\sigma_{xy} \propto q$.

We have proposed a concept of compact topological excitations together with their analytic formulas. We have identified merons as endpoints of stripes in thin chiral magnetic films. A meron has $Q_{\rm sky} = \pm 1/2$ and $Q_{\rm vortex} = 0$ in the easy-axis ferromagnet. This makes a sharp contrast with a meron in the easy-plane ferromagnet, where $Q_{\rm sky} = \pm 1/2$ and $Q_{\rm vortex} = \pm 1$. By neglecting the stripe fluctuations, we have constructed the phase diagram, which is in qualitative agreement with those obtained experimentally and by a Monte Carlo simulation.[8] This demonstrates that our treatment of merons as free particles is a good starting point. It is a future problem to include stripe fluctuations to improve approximation. Magnetic thin films are ideal systems to investigate and test various intriguing ideas on topological excitations.

The author is deeply indebted to Y. Tokura, Y. Onose, X. Z. Yu, and A. Rosch for illuminating discussions and for information on experimental details, and is very grateful to N. Nagaosa and J. H. Han for fruitful discussions on the subject. This work was supported in part by Grants-in-Aid for Scientific Research from the Ministry of Education, Science, Sports, and Culture No. 22740196 and No. 21244053.

[1] *The Multifaced Skyrmions*, edited by G. E. Brown and M. Rho (World Scientific, Singapore, 2010).

[2] C. G. Callan, R. Dashen, and D. J. Gross, Phys. Rev. D **17**, 2717 (1978).

[3] K. Moon, H. Mori, K. Yang, S. M. Girvin, A. H. MacDonald, L. Zheng, D. Yoshioka, and S-C. Zhang, Phys. Rev. B **51**, 5138 (1995).

[4] T. Senthil, A. Vishwanath, L. Balents, S. Schdev, and M. P. A. Fisher, Science **303**, 1490 (2004).

[5] O. A. Tretiakov and O. Tchernyshyov, Phys. Rev. B **75**, 012408 (2007).

[6] R. Hertel and C. M. Schneider, Phys. Rev. Lett. **97**, 177202 (2006).

[7] S. Mühlbauer, B. Binz, F. Jonietz, C. Pfleiderer, A. Rosch, A. Neubauer, R. Georgii, and P. Böni, Science **323**, 915 (2009); W. Münzer, A. Neubauer, T. Adams, S. Mühlbauer, C. Franz, F. Jonietz, R. Georgii, P. Böni, B. Pedersen, M. Schmidt, A. Rosch, and C. Pfleiderer, Phys. Rev. B **81**, 041203 (2010).

[8] X. Z. Yu, Y. Onose, N. Kanazawa, J. H. Park, J. H. Han, Y. Matsui, N. Nagaosa, and Y. Tokura, Nature (London) **465**, 901 (2010).

[9] T. Ogasawara, N. Iwata, Y. Murakami, H. Okamoto, and Y. Tokura, Appl. Phys. Lett. **94**, 162507 (2009).

[10] M. Ezawa, Phys. Rev. Lett. **105**, 197202 (2010).

[11] A. N. Bogdanov and D. A. Yablonskii, Sov. Phys. JETP **68**, 101 (1989); A. Bogdanov and A. Hubert, J. Magn. Magn. Mater. **138**, 255 (1994).

[12] J. H. Han, J. Zang, Z. Yang, J.-H. Park, and N. Nagaosa, Phys. Rev. B **82**, 094429 (2010).

[13] J. Ye, Y. B. Kim, A. J. Millis, B. I. Shraiman, P. Majumdar, and Z. Tešanović, Phys. Rev. Lett. **83**, 3737 (1999); S. D. Yi, S. Onoda, N. Nagaosa, and J. H. Han, Phys. Rev. B **80**, 054416 (2009).

[14] M. Lee, W. Kang, Y. Onose, Y. Tokura, and N. P. Ong, Phys. Rev. Lett. **102**, 186601 (2009); A. Neubauer, C. Pfleiderer, B. Binz, A. Rosch, R. Ritz, P. G. Niklowitz, and P. Boni, *ibid.* **102**, 186602 (2009).

[15] D. Clarke, O. A. Tretiakov, and O. Tchernyshyov, Phys. Rev. B **75**, 174433 (2007).